Proceedings of the 5th International Conference on Materials Chemistry and Environmental Engineering
DOI: 10.54254/2755-2721/136/2025.20990

A Chemical Transport-Damage Model for Concrete under Sulfate Attack

Cheng Zhang[1,a,*], Jian Yang[1], Xiaojie Hua[1]

[1]*School of Safety Science and Engineering, Nanjing University of Science and Technology, Jiangsu, Nanjing, 210094, China*
a. chen-zhang@njust.edu.cn
**corresponding author*

Abstract: Based on the constitutive relationships of materials, this study investigates the two-stage degradation of cement-based materials under sulfate attack and proposes a comprehensive chemico-transport model to analyze the volumetric changes, porosity evolution, and crack development during the erosion process. The research reveals that, in the early stage of sulfate attack, the formation of gypsum and ettringite fills the pores, enhancing the concrete's density and slowing the diffusion of sulfate ions. However, over time, the expansive stresses generated by these products lead to structural damage, promoting the initiation and propagation of cracks. This, in turn, accelerates the penetration of the aggressive sulfate solution into the concrete, intensifying the consumption of internal components. Quantitative analysis of sulfate ion diffusion patterns enables the estimation of gypsum formation and the associated consumption of C_3A, which is crucial for a deeper understanding of the degradation mechanisms of concrete structures in sulfate environments.

Keywords: Chemical Transport-Damage Model, Concrete under Sulfate Attack, Chemico-transport model.

1. Introduction

Over the past few decades, the study of concrete durability has become a critical issue in structural design. Sulfate attack is a complex degradation process that significantly affects concrete durability, involving various chemo-physical processes such as ion diffusion, chemical reactions, volumetric expansion, and crack formation [1,2]. The intrusion of sulfate ions disrupts the pH balance of the pore solution, causing extensive decalcification of calcium hydroxide (C-H) and calcium silicate hydrate (C-S-H), leading to a reduction in the Ca/Si ratio. This process results in the formation of gypsum, which promotes the crystallization of ettringite [3]. These insoluble expansive products fill the pores and, upon reaching a critical threshold, generate expansive stresses that lead to microcracking and expansion in cementitious materials [4,5]. Additionally, the decalcification of gel products weakens the bond strength between the cement paste and aggregate, reducing the macroscopic strength of the concrete [6-8]. These coupled effects ultimately cause structural damage to concrete in sulfate-rich environments.

Currently, most researchers focus on the diffusion and penetration of sulfate ions and the mechanisms of sulfate-induced concrete deterioration. Various studies have simulated the diffusion-reaction process of external sulfate attack (ESA) on concrete. Zou and Qin [9,10] validated a coupled

© 2025 The Authors. This is an open access article distributed under the terms of the Creative Commons Attribution License 4.0 (https://creativecommons.org/licenses/by/4.0/).

DOI: 10.54254/2755-2721/136/2025.20990

model of external sulfate diffusion and chemical reactions, simulating the effects of temperature on chemical reactions and ion diffusion. Their findings demonstrated that higher sulfate concentrations and temperatures promote external erosion conditions, increase the penetration depth of sulfate ions into concrete, and enhance the diffusion and chemical reaction processes. Marchand [11] considered the coupling of ion and liquid transport, as well as the solid-phase chemical equilibrium in partially saturated systems, using a simplified chemical reaction model to simulate multi-factor coupled chemical ion diffusion.

In contrast, fewer studies have employed chemo-mechanical models to describe sulfate attack. During the degradation of concrete, time-dependent volumetric expansion strain is one of the key factors in describing the evolution of mechanical deterioration. Idiart [12] focused on external sulfate attack on concrete specimens at the meso-scale, simulating the effects of discrete cracks on ion transport in concrete based on fracture mechanics laws. Bary [13] developed a chemo-transport-mechanical model, incorporating macroscopic strain parameters derived from the volumetric fraction of ettringite precipitates into mechanical behavior laws, analyzing the local mechanical and diffusion properties of concrete.

In summary, considering multi-factor coupled effects during concrete degradation is essential for predicting and characterizing its sulfate resistance. In this model, concrete is assumed to be a saturated, isotropic, and porous material, with the transport process driven by concentration gradients according to Fick's second law. This study investigates sulfate ion penetration and secondary chemical reactions of hydration products, accounting for the free volume generated by the dissolution of calcium ions from C-H and C-S-H, which increases the diffusion rate of ion transport. Using a meso-scale model, we analyze the effects of calcium ion leaching and volumetric expansion on external sulfate attack from the perspectives of chemical reaction rates, calcium ion leaching rates, and ion transport rates.

2. Model Formulation

2.1. Sulfate Ion Diffusion

In an external sulfate attack (ESA) environment, erosive ions penetrate concrete along with the solution, reacting with calcium ions and other substances within the concrete to form expansive products such as gypsum and ettringite, which deteriorate the durability of the concrete. Studies have shown that the erosion process can be described by Fick's second law, and the sulfate ions consumed by chemical reactions can be solved using chemical reaction kinetics [5,14-16]:

$$\frac{dC_f}{dt} = D_s(x,t)\frac{d^2C_f}{dx^2} + \frac{dC_d}{dt} \quad (1)$$

$$c(x,0) = 0, x \in \ell \quad (2)$$

$$c(0,t) = c_0, c(L,t) = c_0 \quad (3)$$

Where C_f is the concentration of sulfate ions in concrete (mol/m³), x is the cross-sectional position, $D_s(x,t)$ is the diffusion coefficient of sulfate ions in concrete (m²/s), C_d is the concentration of sulfate ions consumed by chemical reactions (mol/m³), c_0 is the boundary concentration of sulfate ions (mol/m³), L is the thickness of the concrete element (m), and ℓ is the cross-sectional area of the concrete element.

2.2. Chemical Reaction Process

As mentioned earlier, sulfate ions primarily damage the concrete structure through chemical reactions with substances inside the concrete. When sulfate ions penetrate the cementitious materials, they react with the hydrated cement paste.

DOI: 10.54254/2755-2721/136/2025.20990

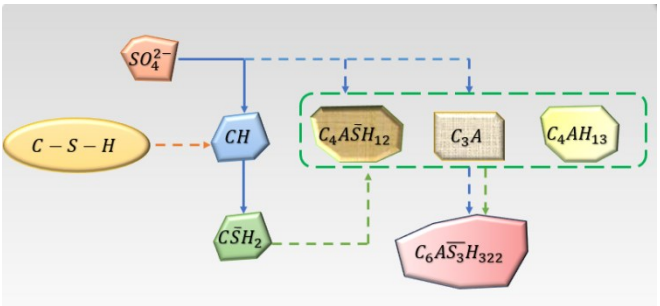

Figure 1: Chemical reaction process of sulfate ions after penetration.

Assuming that the source of sulfate ions is sodium sulfate, the degradation process is initiated by the formation of gypsum ($C\bar{S}H_2$), which is produced by the reaction of sulfate ions with calcium ions dissolved from CH or C-S-H gel:

$$Ca^{2+} + SO_4^{2-} + 2H \rightarrow C\bar{S}H_2 \quad (4)$$

Gypsum ($C\bar{S}H_2$) further reacts with water and unreacted aluminates to form ettringite. As shown in the following equations, the model includes three different calcium aluminate phases (tricalcium aluminate C_3A, tetracalcium aluminate hydrate C_4AH_{13}, and monosulfate AFm). The reaction of tetracalcium aluminate ferrite (C_4AF) with gypsum is assumed to be negligible due to its relatively slow reaction rate:

$$C_3A + 3C\bar{S}H_2 + 26H \rightarrow C_6A\bar{S}_3H_{32} \quad (5)$$

$$C_4AH_{13} + 3C\bar{S}H_2 + 14H \rightarrow C_6A\bar{S}_3H_{32} + CH \quad (6)$$

$$C_4A\bar{S}H_{12} + 2C\bar{S}H_2 + 16H \rightarrow C_6A\bar{S}_3H_{32} \quad (7)$$

Based on previous studies [12,17-18], the formation of ettringite can be concentrated into a single expression:

$$CA + qC\bar{S}H_2 \rightarrow C_6A\bar{S}_3H_{32} \quad (8)$$

Where CA is the equivalent group of reacting calcium aluminates, $CA = \lambda_1 C_3A + \lambda_2 C_4AH_{13} + \lambda_3 C_4A\bar{S}H_{12}$, and $q$is the stoichiometric coefficient of the sulfate phase, with a value of 8/3.

Assuming a second-order chemical reaction in the equation, the depletion rate of sulfate ions, the rate of gypsum formation, and the consumption rate of calcium aluminate can be derived from chemical reaction kinetics:

$$\frac{dC_{SO_4^{2-}}}{dt} = -k_1 C_{SO_4^{2-}} C_{Ca^{2+}} \quad (9)$$

$$\frac{dC_{gpy}}{dt} = k_1 C_{SO_4^{2-}} C_{Ca^{2+}} - k_2 C_{gpy} C_{CA} \quad (10)$$

$$\frac{dC_{CA}}{dt} = -k_2 \frac{C_{gpy} C_{CA}}{q} \quad (11)$$

Where k_1 and k_2 are the reaction rate constants. $C_{Ca^{2+}}$, $C_{SO_4^{2-}}$, C_{gpy} and C_{CA} represent the concentrations of calcium ions, sulfate ions, secondary gypsum, and the equivalent lumped calcium aluminates in the matrix (mol/m³), respectively, and t is the diffusion time. The amount of consumed calcium aluminates is equal to the amount of formed ettringite.

2.3. Calcium Leaching Process

During sulfate attack, the calcium ions that react with sulfate ions primarily originate from the dissolution of calcium hydroxide (CH) and the decalcification of calcium silicate hydrate (C-S-H). This process increases porosity, altering both the transport properties and mechanical performance of the concrete. The amount of calcium ion dissolution influences the rate of chemical reactions.

DOI: 10.54254/2755-2721/136/2025.20990

Calcium leaching is a thermodynamically balanced process that combines diffusion and dissolution. The equilibrium relationship between the calcium ion concentration in the solid phase (C-S-H and CH) and pore solution can be described using a typical solid-liquid equilibrium curve obtained from experimental results. The curve is given by the following equations:

$$C_{ca}^{S}(x,t) =$$

$$\left[\frac{-2}{{x_1}^3}{C_{Ca^{2+}}}^3(x,t)+\frac{3}{{x_1}^2}{C_{Ca^{2+}}}^2(x,t)\right]\left\{C_{CSH0}\left[\frac{C_{Ca^{2+}}(x,t)}{C_{satu}}\right]^{\frac{1}{3}}\right\} \quad 0 \le C_{Ca^{2+}}(x,t) \le x_1 \tag{12}$$

$$\left\{C_{CSH0}\left[\frac{C_{Ca^{2+}}(x,t)}{C_{satu}}\right]^{\frac{1}{3}}\right\} \quad x_1 \le C_{Ca^{2+}}(x,t) \le x_2 \tag{13}$$

$$\left\{C_{CSH0}\left[\frac{C_{Ca^{2+}}(x,t)}{C_{satu}}\right]^{\frac{1}{3}}\right\}+\frac{C_{CH0}}{(C_{satu}-x_2)^3}\left[C_{Ca^{2+}}(x,t)-x_2\right] \quad x_2 \le C_{Ca^{2+}}(x,t) \le C_{satu} \tag{14}$$

Where $C_{ca}^{s}(x,t)$ and $C_{Ca^{2+}}(x,t)$ represent the calcium ion concentrations in the solid phase and the pore solution, respectively. C_{satu} is the saturated calcium ion concentration in the liquid phase (mol/m³), x_1 is the calcium ion concentration (mol/m³) at which C-S-H gel begins to rapidly convert into liquid-phase calcium ions, and x_2 is the calcium ion concentration at which CH is fully dissolved and C-S-H gel begins to dissolve. C_{CSH0} and C_{CH0} are the initial concentrations of calcium in the solid phases of C-S-H and CH (mol/m³), respectively.

The equations describe three stages of the leaching process. Initially, when $C_{Ca^{2+}}(x,t) \le C_{satu}$, CH dissolves rapidly because it has a higher solubility than other hydrates. When $C_{Ca^{2+}}(x,t)$ decreases to x_2, CH is fully dissolved, and the decalcification of C-S-H begins gradually. Further reduction to x_1 causes C-S-H to dissolve rapidly into silica gel, reducing $C_{Ca^{2+}}(x,t)$ to zero [19]. When cement is immersed in corrosive solutions such as ammonium nitrate or sodium chloride, the calcium leaching process accelerates. Consequently, the presence of sulfate ions and their reactions with calcium ions promote the leaching process.Wan et al. found experimentally that the equilibrium curve for a 6000 mol/m³ ammonium nitrate solution is similar to that for water. However, the saturated concentration C_{satu} and the critical concentrations x_1, x_2 increased by two orders of magnitude. According to Phung et al. [20], x_1, x_2, and C_{satu} exhibit a linear relationship with the concentration of the nitrate solution. Due to the lack of reliable data for sulfate solutions, this study assumes that the acceleration of leaching in sulfate solutions is roughly the same as in ammonium nitrate solutions, and that x_1, x_2, and C_{satu} follow a linear relationship with the sulfate solution concentration. The calculation formulas are as follows:

$$x_1 = 2 + \frac{C_{S0}}{S_0}(273-2) \tag{15}$$

$$x_2 = 20 + \frac{C_{S0}}{S_0}(2320-20) \tag{16}$$

$$C_{satu} = 22 + \frac{C_{S0}}{S_0}(2730-22) \tag{17}$$

In the equations, S_0 represents the concentration of the ammonium nitrate solution (6000 mol/m³), and C_{S0} represents the concentration of the sulfate solution.

2.4. Diffusion-Reaction Equations

In the simulation process, the transport within the saturated porous medium is assumed to be driven by concentration gradients and chemical activity gradients, while the influence of the electric

DOI: 10.54254/2755-2721/136/2025.20990

potential is considered negligible. According to Fick's second law and the principle of mass conservation, the ionic transport equation is given by:

$$\frac{dC_i}{dt} = -\mathrm{div}(J_i) + \widetilde{S}_i \tag{18}$$

Where C_i is the concentration of species i in the solution, $\widetilde{S}_i$ is the source term accounting for the formation or consumption of species i, and J_i is the diffusion flux of species , given by:

$$J_i = -D_I\left(\nabla C_i + C_i\nabla \ln\gamma_i + \frac{C_i \ln\gamma_i C_i}{T}\nabla T\right) \tag{19}$$

Where D_I is the diffusion coefficient of ion i in the solution, T is the temperature (K), and the last term in parentheses, ∇T, represents the coupling between solute concentration and the thermal gradient. γ_i is the activity coefficient that accounts for the interactions between various ions Na^+, K^+, Ca^{2+}, OH^- and SO_4^{2-} in the pore solution of concrete. The activity coefficient γ_i is calculated using the modified Davies equation:

$$\ln\gamma_i = -\frac{Az_i^2\sqrt{I}}{1 + a_i B\sqrt{I}} + \frac{\left(0.2 - 0.417 \times 10^{-5} I\right)Az_i^2 I}{\sqrt{1000}} \tag{20}$$

$$I = \frac{1}{2}\sum z_i^2 C_i \tag{21}$$

$$A = \frac{\sqrt{2}F^2 e_0}{8\pi(\varepsilon_k RT)^{\frac{3}{2}}} \tag{22}$$

$$B = \sqrt{\frac{2F^2}{\varepsilon_k RT}} \tag{23}$$

$$\varepsilon_k = \varepsilon_0 \varepsilon_r \tag{24}$$

The symbol z_i denotes the charge number of the ion, and a_i represents the ionic radius (assuming all ionic radii to be 3.0×10^{-10}m). I is the ionic strength of the solution (mol/m³). A and B are temperature-dependent parameters, e_0 is the elementary charge (1.602×10^{-19}C), F is the Faraday constant (96488.6 C/mol), and R is the universal gas constant (8.3143 J/mol·K). ε_k is the dielectric constant of the medium (F/m), ε_0 is the vacuum permittivity (8.85410^{-12}F/m), and ε_r is the relative permittivity of water.

The diffusion-reaction of sulfate ions is described by the following equation, where the source term is represented by the chemical depletion expression. For calcium ions, in addition to depletion due to chemical reactions, the leaching process is considered as the final term in the equation:

$$\frac{dC_{SO_4^{2-}}}{dt} = div\left(D_{SO_4^{2-}}\nabla C_{SO_4^{2-}} + D_{SO_4^{2-}} C_{SO_4^{2-}}\nabla \ln\gamma_{SO_4^{2-}}\right) - k_1 C_{SO_4^{2-}} C_{Ca^{2+}} \tag{25}$$

$$\frac{dC_{Ca^{2+}}}{dt} = div\left(D_{Ca^{2+}}\nabla C_{Ca^{2+}} + D_{Ca^{2+}} C_{Ca^{2+}}\nabla \ln\gamma_{Ca^{2+}}\right) - k_1 C_{SO_4^{2-}} C_{Ca^{2+}} - \frac{dC_{ca}^S}{dt} \tag{26}$$

The initial and boundary conditions for these equations are:

$$initial\ conditions(t = 0): x \in \Omega$$
$$C_{SO_4^{2-}} = 0$$
$$C_{Ca^{2+}} = C_{satu}$$
$$C_{eq} = C_{CA0}$$
$$C_{gyp} = 0$$
$$Boundary\ conditions: x \in \Gamma$$
$$C_{SO_4^{2-}} = C_{S0}$$

DOI: 10.54254/2755-2721/136/2025.20990

$$C_{Ca^{2+}} = 0$$
$$C_{eq} = 0$$
$$C_{gyp} = 0$$

In the equations, C_{S0} and C_{CA0} represent the initial concentrations of the sulfate solution and the equivalent calcium aluminates, respectively. φ_0 is the initial porosity, and Ω and Γ represent the domain and boundary of the specimen, respectively.

2.5. Volumetric Strain

2.5.1. Volumetric Strain Due to Concrete Expansion

According to the chemical reaction equations (4)-(7), the process of volume change in concrete progresses from the dissolution of calcium aluminate hydrates to the formation of ettringite. Due to the presence of initial pores in the concrete and the increase in porosity caused by the dissolution of calcium hydroxide, the ettringite formed gradually fills the pores. Once the pores are sufficiently filled, the concrete begins to expand. Therefore, the volumetric expansion of concrete caused by the growth of ettringite can be expressed as [21]:

$$\varepsilon_{VR} = Max\{(\varepsilon_V - \varepsilon_{\varphi_0} - \varepsilon_{\varphi_{CH}}), 0\} \quad (27)$$

Where ε_{VR} is the actual volumetric strain of the concrete considering the filling of pores by ettringite, ε_V is the volumetric strain without considering pore filling by ettringite, $\varepsilon_{\varphi_{CH}}$ is the reduction in volumetric strain due to the increase in porosity caused by the dissolution of calcium hydroxide, and ε_{φ_0} is the volumetric strain reduction due to the initial porosity.

Without considering the pore-filling effect of ettringite in concrete, the total volumetric strain ε_V due to the dissolution of calcium aluminate hydrates and the formation of ettringite can be expressed as:

$$\varepsilon_V = \frac{1}{V}\sum_{i=1}^{3} \triangle V_{CAi-Ett} \quad (28)$$

Where $\triangle V_{CA1-Ett}$, $\triangle V_{CA2-Ett}$ and $\triangle V_{CA3-Ett}$ represent the volume increments due to the formation of ettringite $C_6A\bar{S}_3H_{32}$ from the chemical reactions involving calcium aluminate hydrates, namely tetra-calcium aluminate hydrate C_4AH_{13}, monosulfate AFm, and tri-calcium aluminate C_3A, respectively. V is the total volume of the concrete (m^3).

$$\varepsilon_V = \sum_{i=1}^{3} \frac{\triangle V_{CAi-Ett}}{V_{CAi}} \cdot \frac{V_{CAi}}{V} = \sum_{i=1}^{3} v_{CAi} \frac{V_{CAi}}{V} \quad (29)$$

Where V_{CA1}、V_{CA2} and V_{CA3} denote the volumes of C_4AH_{13}, AFm and C_3A consumed during the chemical reactions in the concrete (m^3), and v_{CA1}、v_{CA2} and v_{CA3} are the volume change rates of C_4AH_{13}, AFm and C_3A, which are equal to 0.48, 0.55, and 1.31, respectively, according to the chemical reaction equations (5)-(7).

In equation (29), the ratio $\frac{V_{CAi}}{V}$ can be expressed in terms of the concentration of calcium aluminate hydrates consumed due to chemical reactions:

$$\frac{V_{CAi}}{V} = \frac{C_{CAi}}{m_{v-CAi}} \quad (30)$$

DOI: 10.54254/2755-2721/136/2025.20990

Where C_{CA1}、C_{CA2} and C_{CA3} are the concentrations of C_4AH_{13}, AFm, and C_3A consumed by chemical reactions (mol/m³), and m_{v-CA1}、m_{v-CA2} and m_{v-CA3} are the molar volumes of C_4AH_{13}, AFm , and C_3A, which are 3610, 3140, and 11260 mol/m³, respectively.

Combining equation (29), the volumetric strain ε_V due to the dissolution of calcium aluminate hydrates and the formation of ettringite can be expressed as:

$$\varepsilon_V = \sum_{i=1}^{3} v_{CAi} \frac{C_{CAi}}{m_{v-CAi}} \tag{31}$$

Due to the presence of initial pores, a portion of the ettringite produced by the chemical reactions fills the pores, thereby reducing the volumetric expansion of the concrete. Considering the heterogeneity in pore filling by ettringite, the volumetric strain ε_{φ_0} after the reduction of initial porosity can be expressed as a reduction coefficient of the initial porosity [22]:

$$\varepsilon_{\varphi_0} = f \cdot \varphi_w \tag{32}$$

$$\varphi_w = \max\left(f_{vc} \cdot \frac{\frac{w}{c} - 0.36h_\alpha}{\frac{w}{c} + 0.32}, 0 \right) \tag{33}$$

$$f_{vc} = \left[\frac{\rho_c}{\rho_g}\left(\frac{g}{c}\right) + \frac{\rho_c}{\rho_w}\left(\frac{w}{c}\right) + \frac{\rho_c}{\rho_a}\left(\frac{a}{c}\right) \right]^{-1} \tag{34}$$

$$h_\alpha = 1 - 0.5[(1 + 1.67t_s)^{-0.6} + (1 + 0.29t_s)^{-0.48}] \tag{35}$$

Where f is the volume fraction of the initial porosity filled with ettringite, taken as f=0.25; φ_w is the porosity caused by continuous hydration without considering the products of sulfate attack, determined by the above equation; f_{vc} is the volume fraction of cement; w, c, g, and arepresent the masses of water, cement, aggregate, and air, respectively; ρ represents the density of the materials (kg/m³); h_α is the degree of hydration; $\frac{w}{c}$ is the water-to-cement ratio; and t_s is the sum of the concrete curing time and the erosion time.

Through chemical reactions, calcium hydroxide in the concrete continuously dissolves into the pore solution, increasing the porosity of the concrete, thereby reducing the volumetric expansion caused by ettringite filling.

According to chemical reaction equation (10), the volumetric strain of the concrete decreases with increasing porosity, and the reduction in volumetric strain due to the dissolution of calcium hydroxide, $\varepsilon_{\varphi_{CH}}$, is given by:

$$\varepsilon_{\varphi_{CH}} = \frac{C_{Gyp}}{m_{v-CH}} = \frac{1}{m_{v-CH}} \sum_{i=1}^{3} \gamma_i C_{CAi} \tag{36}$$

Where C_{Gyp} is the concentration of secondary gypsum consumed in the reaction, equal to the concentration of secondary gypsum formed; $m_{v-CH} = 29880 \mathrm{mol/m^3}$ is the molar volume of calcium hydroxide, and γ_i are the reaction coefficients corresponding to equations (5)-(7), with γ1=3, γ2=2, and γ3=3.

$$\varepsilon_{VR} = Max\left[\sum_{i=1}^{3} \left(\frac{V_{CAi}}{m_{v-CAi}} - \frac{\gamma_i}{m_{v-CH}} \right) C_{CAi} - f \cdot \varphi_w, 0 \right] \tag{37}$$

To simplify the calculation, let C_{CA1}、C_{CA2} and C_{CA3} represent the molar concentration of the C_4AH_{13}, AFm, and C_3A , respectively

DOI: 10.54254/2755-2721/136/2025.20990

$$C_{CA} = \sum_{i=1}^{3} C_{CAi} \approx qC_{CAi}\,(i = 1,2,3) \tag{38}$$

Substituting equation (38) into equation (37), the volumetric strain caused by ettringite growth can be expressed as:

$$\varepsilon_{VR} = Max\left[\frac{1}{q}\sum_{i=1}^{3}\left(\frac{v_{CAi}}{m_{v-CAi}} - \frac{\gamma_i}{m_{v-CH}}\right)C_{CA} - f\cdot\varphi_w, 0\right] \tag{39}$$

The pore-filling effect of ettringite influences the porosity of the concrete, and the porosity filled by ettringite can be obtained by:

$$\varphi_{fill} = Min\left[\frac{1}{q}\sum_{i=1}^{3}\left(\frac{v_{CAi}}{m_{v-CAi}} - \frac{\gamma_i}{m_{v-CH}}\right)C_{CA}, f\cdot\varphi_w\right] \tag{40}$$

In summary, the filling of pores by sulfate products reduces the porosity of the concrete, and the porosity during the diffusion and chemical reaction of sulfate ions in the concrete can be expressed as:

$$\varphi = \left[Max\left(\varphi_w - \varphi_{fill}\right), 0\right] \tag{41}$$

2.5.2. Establishment of the Crack Damage Function

The degradation process of concrete in sulfate solutions is highly complex. Therefore, describing the microstructural changes caused by erosion products during the erosion process using a damage function can help to better understand the damage evolution of concrete under the effect of external sulfate attack (ESA).

A time-dependent function can be constructed to represent the development of concrete damage under the influence of ESA:

$$D(t) = 1 + d \tag{42}$$

Where D(t) is the damage function, and d represents the degree of damage to the concrete.

The degree of damage is defined as the change in a parameter of the concrete (such as elastic modulus, compressive strength, etc.) after erosion compared to its pre-erosion state. Taking the elastic modulus as an example, the degree of damage can be expressed as:

$$d = \frac{\Delta E}{E_0} = \frac{E_0 - E_t}{E_0} = 1 - \frac{E_t}{E_0} = 1 - \mu(t) \tag{43}$$

where E_0 and E_t are the initial elastic modulus of the concrete and the elastic modulus after t days of erosion, respectively. μ(t) is an intermediate function related to damage. The relationship between μ(t) and 1 reflects the increase or decrease in the elastic modulus before and after erosion. The following is an analysis of the factors affecting μ(t).

First, the continuous hydration reaction improves the internal structure of the concrete, resulting in an increase in μ(t). This parameter is denoted as $f_H(t)$:

$$f_H(t) = \frac{1}{1 - a_H\left[1 - \exp\left(-b_H\frac{t}{730}\right)\right]} \tag{44}$$

where f_H represents the effect of hydration on the damage of concrete, and a_H and b_H are experimental parameters obtained from fitting experimental data. t_0 is the hydration curing time, and t is the erosion time.

Next, the influence of the erosion products on the development of damage during ion diffusion is considered. The evolution of concrete performance under sulfate immersion can be divided into two stages: a short-lived improvement due to pore filling and an accelerated damage process due to

DOI: 10.54254/2755-2721/136/2025.20990

cracking. These two stages correspond to an increase and a decrease in μ(t), respectively, which are denoted as $f_E(t)$ and , $f_D(t)$:

$$f_E(t) = a_E\left[1 - \exp\left(-b_E\frac{t}{730}\right)\right] \tag{45}$$

$$f_D(t) = a_D\left(\frac{t}{730}\right)^{b_D} \tag{46}$$

where f_E and f_D represent the increase and decrease of μ(t) in the two stages, respectively. a_E、b_E、a_D and b_E are experimental parameters obtained from fitting experimental data. The following conditions must be satisfied by the equations:

$$f_H(0) = 1$$
$$f_D(0) = f_E(0) = 0$$
$$f_D(t) \le f_H(t) + f_E(t) \tag{47}$$

Based on the effects of f_H、f_E and f_D on μ(t), and following the method in reference [23], μ(t) can be defined as:

$$\mu(t) = [f_H(t) + f_E(t)] \cdot [1 - f_D(t)] \tag{48}$$

Substituting μ(t) into the previous equation, the expression for the degree of damage ddd is obtained as:

$$d = 1 - \mu(t) = 1 - [f_H(t) + f_E(t)] \cdot [1 - f_D(t)] \tag{49}$$

When $\mu < 1$, indicating a decrease in the elastic modulus and the destruction of the internal structure of the concrete, which accelerates the diffusion of ions. Conversely, when $\mu > 1$, $d < 0$, indicating an increase in the elastic modulus and the filling of pores within the concrete, which slows down the diffusion of ions. In summary, the expression for D(t) is:

$$D(t) = 1 + \mathrm{d} = 2 - [f_H(t) + f_E(t)] \cdot [1 - f_D(t)] \tag{50}$$

The dimensionless parameters involved in the equation are shown in Table 1 [24]. These parameters are derived by converting the ultrasonic wave propagation speed and density of the concrete before and after sulfate erosion.

Table 1: Parameter values of damage function

w/c	a_H	b_H	a_E	b_E	a_D	b_D
0.7	0.2317	42.73	1.085	0.3443	0.2627	0.3469
0.6	0.1828	38.14	8.5	0.0809	0.3912	0.9338
0.4	0.1293	31.73	0.1589	2.999	2.418	1.204

2.6. Correction of the Diffusion Coefficient

The diffusion coefficient is a crucial parameter in diffusion models as it effectively describes the movement of various ions within a concrete structure. Considering the influence of the material composition and environmental conditions on performance, the diffusion coefficient changes over time due to factors such as material degradation. To ensure a more realistic representation of ion diffusion, it is necessary to correct the diffusion coefficient. At the initial stage of sulfate ion erosion, the formation of gypsum and ettringite fills microcracks, making the concrete denser and reducing its porosity. However, as erosion products accumulate, the cracks eventually stop acting as a buffer, and the resulting expansion stress promotes the creation and propagation of more cracks. The increased porosity facilitates the diffusion of various ions.

Based on the microstructure of concrete, the properties of the three phases—aggregate, mortar, and the interfacial transition zone (ITZ)—are different, and their corresponding diffusion coefficients

DOI: 10.54254/2755-2721/136/2025.20990

vary. It is generally believed that the density of the aggregate is high, and it is not corroded by sulfate solutions, so the diffusion coefficient of sulfate ions inside the aggregate is considered to be zero. The diffusion coefficients for the mortar and the ITZ are affected by factors such as the water-cement ratio and the degree of hydration, and the diffusion coefficient of the ITZ is larger than that of the mortar. Therefore, the diffusion coefficient of sulfate ions is mainly derived from the mortar and the ITZ phases.

(1) Mortar Diffusion Coefficient

Considering the effects of porosity, tortuosity, and erosion damage on sulfate ion transport, the diffusion coefficient can be expressed by the following equation [25]:

$$D_S = \frac{[\varphi + D(t)]}{\tau} D_{s0} \tag{51}$$

where D(t) is the damage function describing the damage caused by sulfate erosion, D_{s0} is the initial diffusion coefficient of sulfate ions in cement mortar, which is $3.5 \times 10^{-10} m^2/s$[26], and τ is the tortuosity of the concrete. The tortuosity of concrete is defined as the ratio of the actual diffusion distance to the shortest distance.

$$\tau = \eta_s \eta_a \left(1 + 0.35\sqrt{f_s}\right)\left(1 + 0.35\sqrt{f_a}\right)\tau_{cp} \tag{52}$$

where τ is the tortuosity of the transport path in the pore space of concrete, η_s and η_a are the shape factors of the equivalent spherical particles of sand and aggregate, respectively, f_s and f_a are the volume fractions of sand and coarse aggregate, which can be calculated from the concrete mix ratio. τ_{cp} is the tortuosity of the transport path in the hardened cement paste and can be expressed as:

$$\tau_{cp} = \omega_{wc} \eta_r h_\alpha \frac{1}{1 - \sqrt{1 - \varphi_0}} \sqrt{\left(1 - \sqrt{1 - \varphi_0}\right)^2 + 0.25} \tag{53}$$

$$\omega_{wc} = (1 + 7h_\alpha)^{\frac{w}{c} - 0.35} \tag{54}$$

where ω_{wc} is the correction factor for the effect of the water-cement ratio on the tortuosity of the hardened cement paste [27], η_r is the shape factor of the cement particles, and φ_0 is the initial porosity.

(2) ITZ Diffusion Coefficient

The interfacial transition zone (ITZ) plays a crucial role in the transport properties of cementitious materials. This region contains higher porosity, a larger pore structure, and a higher volume fraction of $Ca(OH)_2$. It is known that the permeability of concrete is higher than that of its cement paste matrix, indicating the dominant role of the ITZ [28]. The diffusion coefficient of the ITZ is 6 to 12 times that of the cement paste [30]. In this study, the diffusion coefficient of the ITZ is chosen as $6D_S$.

3. Simulation Results and Discussion

3.1. Numerical Example

In this study, the Comsol Multiphysics PDE module was used to simulate the sulfate ion erosion process in concrete. The model consists of a concrete specimen with dimensions of 100 mm × 100 mm × 100 mm, immersed in a 3% sodium sulfate solution. To observe the ion transport process more clearly, only one face of the specimen is subjected to erosion, while the other five faces are covered with epoxy resin. The specific parameters used in the simulation are shown in Table 2.

Table 2: The main parameter in the model

parameter	value	reference
C_{CA0}	$63.57 mol/m^3$	Initial concentration of calcium aluminate[9]
C_{CH0}	$1135 mol/m^3$	Initial concentration of CH[9]

DOI: 10.54254/2755-2721/136/2025.20990

Table 2: (continued).

C_{CSH0}	$1049 mol/m^3$	Initial concentration of C-S-H[9]
k_1	$1.22 \times 10^{-8} m^3/mol/s$	Chemical reaction rate constant[30]
k_2	$1.22 \times 10^{-9} m^3/mol/s$	Chemical reaction rate constant[30]
ρ_c	$3100 kg/m^3$	Cement density
ρ_g	$2500 kg/m^3$	Aggregate density
ρ_a	$1.3 kg/m^3$	Air density
$\frac{w}{c}$	0.4	Water-cement ratio
φ_0	0.1206	Initial porosity

3.2. Sulfate Ion Distribution

In the simulation of sulfate ion diffusion within concrete, the model takes into account two key phenomena: the accelerated diffusion rate caused by decalcification reactions during the early stages of exposure, and the pore-filling effects of ettringite formation at later stages. To obtain the distribution of sulfate ions, the diffusion-reaction equation for sulfate ions is solved, incorporating the dynamics of both diffusion and chemical reactions.

Figure 2 presents the sulfate ion concentration distribution across the cross-section of the concrete specimen under varying boundary conditions and at different diffusion times. From the figure, it is evident that when the specimen is immersed in a 3% sodium sulfate solution, the concentration of sulfate ions increases as the diffusion time extends. Notably, the rate of concentration increase is not uniform; it is more pronounced near the surface of the specimen and diminishes progressively towards the interior. This gradient in the rate of increase is due to the higher availability of sulfate ions and reactive sites at the surface, which facilitates faster initial penetration.

As the diffusion time continues to increase, the rate of sulfate ion penetration into the concrete gradually slows down. This deceleration is partly due to the saturation of reactive sites and the formation of ettringite, which fills the pores and reduces the permeability of the concrete. The chemical reaction rate, which initially lags behind the diffusion rate due to the presence of unreacted calcium aluminate and calcium hydroxide, eventually catches up. At this stage, the system reaches a state of dynamic equilibrium, where the rate of sulfate ion diffusion into the concrete matches the rate at which these ions are consumed through chemical reactions, primarily the formation of ettringite and gypsum.

In this dynamic equilibrium, the internal erosion depth of the concrete continues to increase, albeit at a slower pace than in the initial stages. The steady-state condition indicates that while the concrete is still undergoing erosion, the rate of degradation has stabilized. This equilibrium phase is critical for understanding the long-term durability and performance of concrete in sulfate-rich environments, as it provides insight into the ultimate depth of penetration and the degree of structural damage that can be expected over extended periods of exposure.

DOI: 10.54254/2755-2721/136/2025.20990

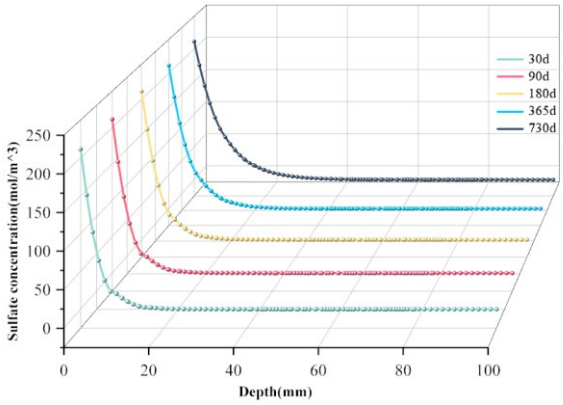

Figure 2: Concentration changes with position and time(3%).

Table 3: Erosion Depth in 3% Na_2SO_4 Solution

Time(d)	30	90	180	365	730
Depth(mm)	19.54	20.76	23.43	28.67	39.39

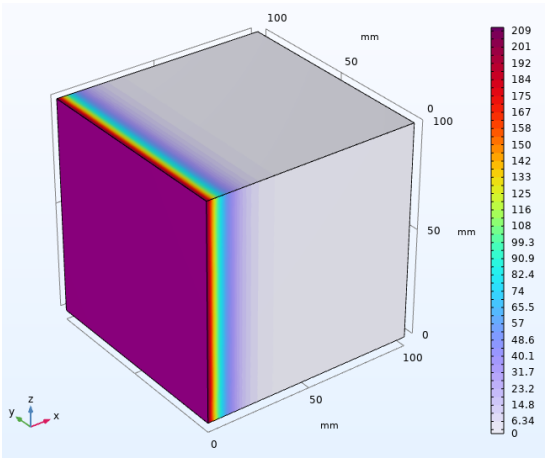

Figure 3: Concentration Distribution of Sulfate Ion Erosion in Concrete (720 days).

3.3. Sulfate Ion Dissipation Distribution

A portion of the sulfate ions that diffuse into the concrete matrix undergoes a series of chemical reactions, starting with their interaction with calcium hydroxide ($Ca(OH)_2$) to form gypsum ($CaSO_4 \cdot 2H_2O$). Subsequently, the gypsum reacts with calcium aluminate (C_3A) to produce ettringite, a needle-like crystalline compound known for its expansive nature. The extent to which sulfate ions dissipate throughout the concrete is crucial in determining the quantity of gypsum produced, and consequently, the amount of C_3A consumed. This information can be utilized to estimate the formation of ettringite, which plays a key role in the degradation of concrete structures exposed to sulfate-rich environments.

The dissipation of sulfate ions, a critical parameter in assessing the progress of sulfate attack, can be quantitatively evaluated using Equation (10), which models the diffusion process based on factors such as the diffusion coefficient, time, and the geometry of the concrete sample. Figure 4 graphically represents the sulfate ion dissipation as a function of the cross-sectional position within the concrete and the duration of exposure to the sulfate solution. It clearly shows that, as the diffusion time

DOI: 10.54254/2755-2721/136/2025.20990

increases, the extent of sulfate ion dissipation also rises, creating a gradient that decreases from the surface toward the inner regions of the concrete. This gradient reflects the fact that the surface of the concrete, being in direct contact with the sulfate-rich environment, experiences a higher influx of sulfate ions compared to its core.

At the critical point of erosion depth, the situation becomes more complex. Here, despite the ongoing structural damage and the continuous influx of sulfate ions, the change in sulfate ion concentration tends to reach a steady state. This stabilization is indicative of a dynamic equilibrium where the rate of sulfate ion entry matches the rate of their chemical conversion into gypsum and ettringite. Both the free and bound sulfate ion concentrations exhibit a similar trend, showing a decrease with increasing depth into the concrete. This observation suggests that the chemical reactions involving sulfate ions are more advanced in zones with a higher initial concentration of these ions, such as the outer layers of the concrete. As a result, the formation of ettringite and the associated physical stresses are more pronounced in these regions, potentially leading to the development of cracks and the overall deterioration of the concrete's mechanical properties.

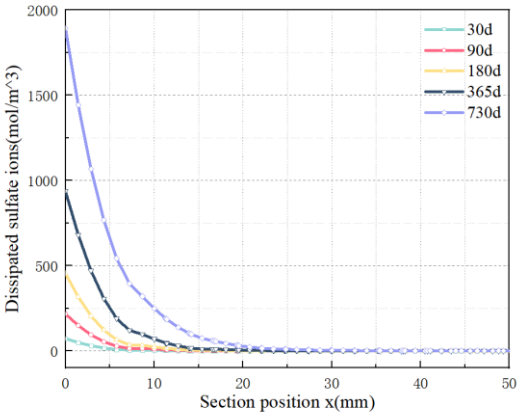

Figure 4: Concentration of gyp at different attack time.

3.4. Calcium Aluminate Dissipation Distribution

In this study, the initial concentration of calcium aluminate (C_3A) in the concrete was set at 63.57 mol/m^3.Figure 4 illustrates the progressive depletion of C_3A over time and across different cross-sectional positions within the concrete. As sulfate ions (SO_4^{2-}) penetrate the concrete, they react with C_3A to form ettringite (AFt), leading to the gradual consumption of C_3A. By comparing data from various time points, it is evident that the rate of this reaction is particularly rapid during the early stages of erosion.

During the initial phase of erosion, the interaction between SO_4^{2-} and C_3A results in the formation of ettringite, an expansive product. This process initially enhances the structural integrity of the concrete by reducing porosity and slowing down the diffusion rate of sulfates. Consequently, in the early stages, the remaining C_3A concentration increases linearly with distance from the surface. However, as erosion progresses, the crystallization pressure exerted by ettringite and other expansion products begins to compromise the structural integrity of the concrete. Cracks start to form and propagate towards the surface, which in turn accelerates the penetration of the erosive medium and intensifies the consumption of C_3A.

Furthermore, Figure 6 highlights the spatial distribution characteristics ofC_3A depletion. In the early stages of erosion, areas near the surface, where the concentration of SO_4^{2-} is higher, experience a faster rate of C_3A consumption. With continued erosion, this depletion pattern gradually extends

DOI: 10.54254/2755-2721/136/2025.20990

deeper into the concrete. Although, at first, the formation of ettringite helps to fill pores and increase the density of the concrete, this positive effect is temporary. Over time, the continuous generation of ettringite and other expansive products leads to significant internal stress within the concrete, ultimately resulting in structural damage.

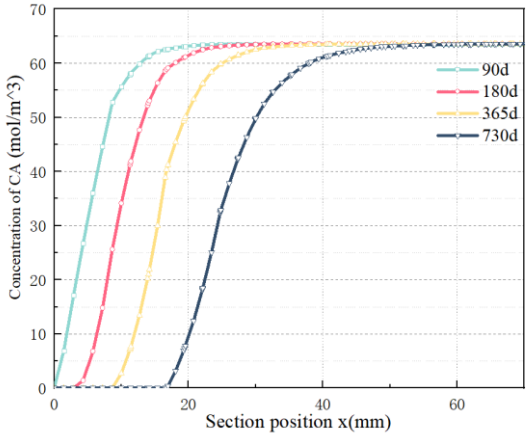

Figure 5: Concentration of CA at different attack time.

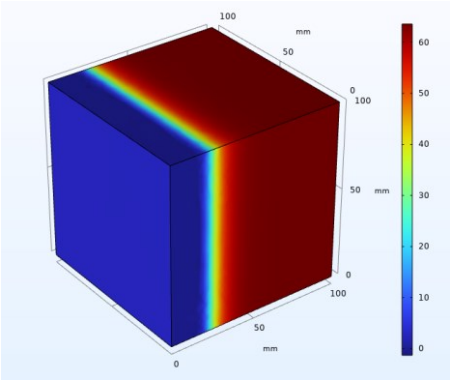

Figure 6: Calcium Aluminate Dissipation and Remaining Concentration Distribution (730 days)

4. Conclusion

This study delves into the impact of sulfate attack on the durability of concrete, elucidating a two-phase evolution of concrete performance: an initial phase characterized by temporary improvement in density due to the filling of pores with gypsum and ettringite, followed by a phase of accelerated deterioration marked by crack propagation. By employing a chemico-transport model, we have analyzed the volumetric changes, porosity evolution, and crack development during the erosion process. It was found that the early stages of sulfate attack lead to an increase in concrete density as the formation of gypsum and ettringite fills the pores, which initially slows down the diffusion of sulfate ions. However, as the duration of exposure increases, the expansive pressure generated by these chemical products initiates structural damage, leading to the formation and propagation of cracks. This, in turn, facilitates deeper penetration of the erosive medium, accelerating the depletion of internal components.

Based on these findings, we have developed a set of mathematical expressions to quantitatively describe the progression of damage in concrete under sulfate attack conditions. These models effectively capture the interrelationships between erosion depth, porosity changes, and crack propagation. The results not only enhance our understanding of the mechanisms behind sulfate-

DOI: 10.54254/2755-2721/136/2025.20990

induced degradation but also provide a robust framework for predicting the long-term performance of concrete in sulfate-rich environments. By fine-tuning the model parameters, it is possible to accurately simulate the erosion behavior of concrete under various environmental conditions, offering valuable insights for optimizing mix designs and developing effective protective measures against sulfate attack.

References

[1] *Ragoug R, Metalssi O O, Barberon F, et al. Durability of cement pastes exposed to external sulfate attack and leaching: Physical and chemical aspects[J]. Cement and concrete research, 2019, 116: 134-145.*

[2] *Yin G J, Zuo X B, Sun X H, et al. Macro-microscopically numerical analysis on expansion response of hardened cement paste under external sulfate attack[J]. Construction and Building Materials, 2019, 207: 600-615.*

[3] *Cefis N, Comi C. Chemo-mechanical modelling of the external sulfate attack in concrete[J]. Cement and Concrete Research, 2017, 93: 57-70.*

[4] *Ikumi T, Segura I. Numerical assessment of external sulfate attack in concrete structures. A review[J]. Cement and Concrete Research, 2019, 121: 91-105.*

[5] *Sun C, Chen J, Zhu J, et al. A new diffusion model of sulfate ions in concrete[J]. Construction and Building Materials, 2013, 39: 39-45.*

[6] *Yu Y, Zhang Y X. Numerical modelling of mechanical deterioration of cement mortar under external sulfate attack[J]. Construction and Building Materials, 2018, 158: 490-502.*

[7] *Liu T, Zou D, Teng J, et al. The influence of sulfate attack on the dynamic properties of concrete column[J]. Construction and Building Materials, 2012, 28(1): 201-207.*

[8] *Liu T, Qin S, Zou D, et al. Experimental investigation on the durability performances of concrete using cathode ray tube glass as fine aggregate under chloride ion penetration or sulfate attack[J]. Construction and Building Materials, 2018, 163: 634-642.*

[9] *Zou D, Qin S, Liu T, et al. Experimental and numerical study of the effects of solution concentration and temperature on concrete under external sulfate attack[J]. Cement and Concrete Research, 2021, 139: 106284.*

[10] *Qin S, Zou D, Liu T, et al. A chemo-transport-damage model for concrete under external sulfate attack[J]. Cement and Concrete Research, 2020, 132: 106048.*

[11] *Marchand J, Samson E, Maltais Y, et al. Theoretical analysis of the effect of weak sodium sulfate solutions on the durability of concrete[J]. Cement and Concrete Composites, 2002, 24(3-4): 317-329.*

[12] *Idiart A E, López C M, Carol I. Chemo-mechanical analysis of concrete cracking and degradation due to external sulfate attack: A meso-scale model[J]. Cement and Concrete Composites, 2011, 33(3): 411-423.*

[13] *Bary B, Leterrier N, Deville E, et al. Coupled chemo-transport-mechanical modelling and numerical simulation of external sulfate attack in mortar[J]. Cement and Concrete Composites, 2014, 49: 70-83.*

[14] *Zhang C, Chen W, Mu S, et al. Numerical investigation of external sulfate attack and its effect on chloride binding and diffusion in concrete[J]. Construction and Building Materials, 2021, 285: 122806.*

[15] *Meng Z, Liu Q, Ukrainczyk N, et al. Numerical study on the chemical and electrochemical coupling mechanisms for concrete under combined chloride-sulfate attack[J]. Cement and Concrete Research, 2024, 175: 107368.*

[16] *Qiao HX, Qiao GB, Lu CG.. Damage and deterioration model of concrete based on COMSOL in sulfate environment[J]. 2021.*

[17] *Yin G J, Zuo X B, Sun X H, et al. Macro-microscopically numerical analysis on expansion response of hardened cement paste under external sulfate attack[J]. Construction and Building Materials, 2019, 207: 600-615.*

[18] *Tixier R, Mobasher B. Modeling of damage in cement-based materials subjected to external sulfate attack. I: Formulation[J]. Journal of materials in civil engineering, 2003, 15(4): 305-313.*

[19] *Wan K, Li L, Sun W. Solid–liquid equilibrium curve of calcium in 6 mol/L ammonium nitrate solution[J]. Cement and concrete research, 2013, 53: 44-50.*

[20] *Phung Q T, Maes N, Jacques D, et al. Modelling the evolution of microstructure and transport properties of cement pastes under conditions of accelerated leaching[J]. Construction and Building Materials, 2016, 115: 179-192.*

[21] *Zuo X B. Modeling ion diffusion-reaction behavior in concrete associated with durability deterioration subjected to couplings of environmental and mechanical loadings[J]. Nan**g, School of Materials Science and Engineering, Southeast University, 2011.*

[22] *Tixier R, Mobasher B. Modeling of damage in cement-based materials subjected to external sulfate attack. II: Comparison with experiments[J]. Journal of materials in civil engineering, 2003, 15(4): 314-322.*

[23] *Chen J, Jiang M, Zhu J. Damage evolution in cement mortar due to erosion of sulphate[J]. Corrosion Science, 2008, 50(9): 2478-2483.*

DOI: 10.54254/2755-2721/136/2025.20990

[24] Jin LB, Wang Z, Yang B, et al. Mesoscopic numerical simulation of sulfate ion transport behavior in concrete based on a new damage model[C]//Structures. Elsevier, 2024, 61: 106066.

[25] Zhuang Y, Liu X, Zhou X, et al. Diffusion model of sulfate ions in concrete based on pore change of cement mortar and its application in mesoscopic numerical simulation[J]. Structural Concrete, 2022, 23(6): 3786-3803.

[26] Zuo Xiaobao, Sun Wei. Full process of concrete damage and failure under sulfate erosion [J]. Journal of Silicate Studies, 2009, 37(7): 1063-1067.

[27] Guan Bowen, Liu Jianan, Wu Jiayu, et al. Sulfate ion transport behavior in concrete based on erosion damage [J]. Bulletin of Silicate, 2020, 39(10): 3169-3174.

[28] Young J F. Review of the pore structure of cement paste and concrete and its influence on permeability[J]. Special Publication, 1988, 108: 1-18.

[29] Bourdette B, Ringot E, Ollivier J P. Modelling of the transition zone porosity[J]. Cement and concrete research, 1995, 25(4): 741-751.

[30] Zuo X B, Sun W, Yu C. Numerical investigation on expansive volume strain in concrete subjected to sulfate attack[J]. Construction and Building Materials, 2012, 36: 404-410.